FUSION ALGORITHM OF OPTICAL IMAGES AND SAR WITH SVT AND SPARSE REPRESENTATION

Yin Zhouping

School of Computer and Information, AnQing Normal University, Anqing 246011, Anhui, China

Submitted: Jan. 30, 2015 ***Accepted: Apr. 12, 2015*** ***Published: June 1, 2015***

Abstract- Due to the different imaging mechanism of optical image and Synthetic Aperture Radar (SAR) image, they have the large different characteristics between the images, so fusing optical image and SAR image with image fusion technology could complement advantages and be able to better interpret the scenes information. A fusion algorithm of Synthetic Aperture Radar and optical image with fast sparse representation on low-frequency images was proposed. For the disadvantage of target information easily missing and the contrast low in fused image, and the fusion method with sparse representation could effectively retain target information of Synthetic Aperture Radar image, so the paper fuses low frequency images of Synthetic Aperture Radar and optical images using sparse representation. Moreover a new sparse coefficient fusion rules is proposed, and sparse decomposition process is improved to reduce the algorithm running time. Experimental results demonstrate the effectiveness of the algorithm.

Index terms*:* fusion algorithm, SAR, optical images, sparse representation, algorithm running time, Support Value Transform.

I. INTRODUCTION

As the different imaging mechanism of optical image and Synthetic Aperture Radar（SAR) image, having the large different characteristics between images, so fusing two types of images with image fusion technology could complement advantages and be able to better interpret the scenes information. However, information reflecting the goals of the two types of images is very different; it is difficult to obtain great fusion effect with conventional methods, so few research currently underway among the two types of image. This paper studies the fusion of two types of images for the purpose of target recognition with Support Value Transform (SVT) transform and sparse representation, analyzed the relevance and synergy between pixel level and feature level fusion algorithm, presented a mixed fusion algorithm between the two types of images, established a multi-level mixed color image fusion model with color information processing and gray image colorization method [1].

In recent years, with the development of mathematical theory, a variety of digital image transformation methods are proposed, multi-scale transform (MST) method has become a research hot spot. MST method includes Laplace Pyramid decomposition, discrete wavelet transforms (DWT) [2,3], contourlet transform (Contourlet), non-down-sampled contourlet transform (NSCT) [4] and the support value transforms (SVT) [5]. Pyramid transform is through continuous filter and down sample the image to get the decomposition structure of the pyramid forms, and the structure is related to each other in different scales sparse, and the robustness of the algorithm is not good. Wavelet transform is a further study of the pyramid decomposition, and it can be decomposed in different scales for the image, and it is able to capture the image details, and it is suitable to represent the isotropic characteristics of the point singularity , but the characteristics of anisotropic representation is bad. Contourlet transform is a ' real representation of two-dimensional image', in the transformation process of multi-scale and multidirectional decomposition is carried out separately, so it has the multi-scale and time-frequency local characteristic, but also has a high degree of directionality and anisotropy, but due to the presence of up-sampling and down-sampling operation at transformation process [6]. Contourlet is lack of shift invariance; the spectrum has the aliasing phenomenon. NSCT is the further optimization of Contourlet transform inherited the good characteristics of Contourlet transform, and it also has the shift invariance, but the algorithm is complex, and the calculating speed is slow. SVT is the least squares support

vector machine (LS-SVM). Based on this, a non sampling value of two redundant transform is a kind of new multi-scale transform method. Through the support value transform for the image, we can get a series of low frequency and high frequency coefficients like other multi-scale decomposition, the low frequency coefficients of the source images is 'approximate' expression, and the high frequency coefficients are an effective representation for image texture details, and it has the very good translation in variance, won't produce ringing effect, speed of operation soon, the multi-scaled composition method used in this paper [7-10, 30-31].

The author has been to build on the initial SAR segmentation to produce a low-level description of the SAR scene and then to demonstrate the use of high-level processing applied to the low-level components [27]. Multi source image fusion is the image obtained from multiple sensors in the fusion, and it is currently a research trend. Benjamin W M and Ranga R V[11] researched on the interest region of multi-source remote sensing image (mainly SAR and multi optical images) fusion algorithm, Yao W [12] did fusion research on TM image and SAR image, Xing S X [13] proposed the fusion algorithm of the optical image and infrared remote sensing image. These fusion algorithms are fusion for the gray level of two remote sensing images, and the fusion process is not a purpose, such as the common optical image and infrared image fusion, optical image and SAR image fusion, the fusion image is obtained for the gray image, target identification and recognition effect. Study on infrared image, optical image and SAR image are still very rare. Aiming at this problem, this paper is intended to target recognition, discusses the fusion algorithm between optical image and SAR image, a two image multilevel mixed color fusion model is set up in order to enhance the image of information description and target recognition effect [14-16, 28]. The paper in [29] focuses on the shadow region in the SAR image by synthetic aperture. Also, the author analyzed the blurred boundary by imaging formation theory.

The rest of this paper is organized as follows. In Section 2, the framework of fusion algorithm is briefly reviewed. Section 3 describes the overcomplete sparse representation in details. Section 4 describes the proposed image fusion algorithm in detail. The experiment results and discussions are presented in Section 5. Finally, we draws a conclusion in Section 6.

II. FRAMEWORK OF FUSION ALGORITHM

Synthetic Aperture Radar (SAR) and optical images are multiscale decomposed, and the approximate number of zero is rarely in the low frequency sub band coefficients, namely the sparsely is small, and the expression of low-frequency information of images is not valid [17]. Overcomplete dictionary can be expressed more sparse image compared with the multiscale decomposition, and it can effectively extract the potential information of images and low frequency [18], but it is not easy in the fusion image edge and texture details. Therefore this paper presents a multi-scale decomposition and sparse representation algorithm combining SAR and optical images. First, the source images are done multi-scale decomposition based on SVT, and then the low-frequency sub-band images are decomposed, sparse representation of high frequency sub-band image by fusion based on regional energy, finally, the fusion image is obtained by reconstruction. The algorithm process is shown in Fig.1.

This paper focuses on the low frequency algorithm based on sparse representation of images fusion, and the treatment of zero mean image block greatly enhances ‘sparse coding’ efficiency, and a new fusion rule propose based on a weighted average and l_1 norm for sparse coefficient is proposed. Experimental results demonstrate the effectiveness of the proposed algorithm.

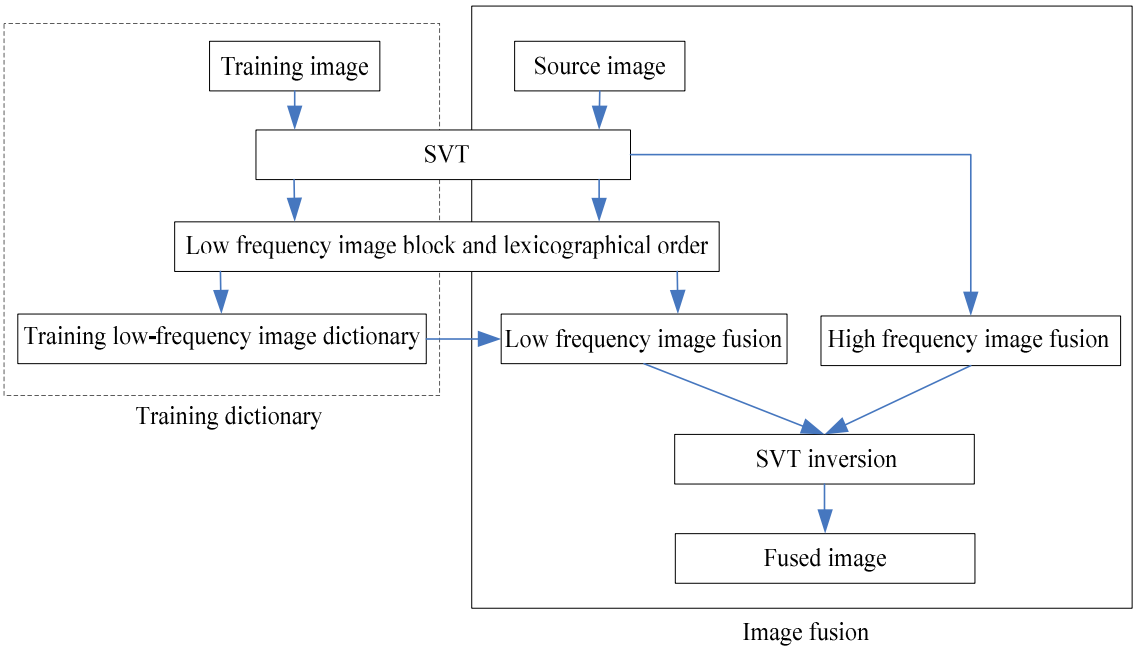

Fig. 1 Flow chart of images fusion algorithm

III. OVERCOMPLETE SPARSE REPRESENTATION

3.1 Images sparse representation

Image sparse representation of orthogonal basis function is adopted to replace the traditional overcomplete basis, and seek a few elements in the overcomplete basis to represent the image feature. Due to the big redundancy based on the basis function and therefore it has better expressing ability [19]. For a signal with $y \in R^{n\times 1}$, the sparse representation can be obtained by solving formula (1) to get the optimal solution:

$$\min\left\|x\right\|_0^0 \qquad s.t\left\|y - Dx\right\|_2 \le \varepsilon \tag{1}$$

Where $D \in R^{n\times K}$ is overcomplete dictionary, and each column represents an atom in the dictionary, $x \in R^{K\times 1}$ is sparse coefficient vector, $\left\|x\right\|_0^0$ represents the number of nonzero elements in the vector x, ε is allowable error. Optimization on the type of process is also known as 'sparse coding'.

Theoretically, we can obtain a sparse representation of the image, but this will lead to large atomic size in the dictionary, and the computational complexity is greatly increased, and the local information of image fusion is dependent on the source image, so in the actual fusion process we use a sliding window to the source image divided into blocks, for sparse image block representation, by processing the image block sparse coefficient to achieve the ultimate source image fusion. This paper takes the source image divided into 8×8 blocks[20] .

Image sparse representation consists mainly of dictionary and sparse representation algorithm, and this paper uses K-SVD algorithmto construct the training dictionary, and the method alternates executing the update procedure of the atomic and the sparse representation of the current dictionary to achieve the purpose of learning the dictionary [21]. Using the orthogonal matching pursuit (OMP) computes sparse decomposition coefficient [22].

3.2 Training algorithm of K-SVD dictionary

This paper constructs the training dictionary by using K-SVD algorithm in the low frequency image of SVT decomposition, and the training dictionary can been obtained by the solution of formula (2):

$$\arg\min_{D,X}\left\|Y-DX\right\|_F^2 \qquad s.t. \qquad \left\|x_i\right\|_0^0 \le T, \forall i \tag{2}$$

Where, $Y=[y_1, y_2 \cdots y_N] \in R^{n\times N}$ is the training sample set, i.e. the set of the training image block; $X \in R^{K\times N}$ is the sparse coefficient matrix, x_i is the $i-th$ column of X; T is the sparse degree.

If the dictionary D is sure, the sparse coefficient of Y sample set in formula (2) can be obtained by OMP algorithm, and then the atom of the dictionary D is revised by these sparse coefficients, namely the columns of the matrix. Assuming the sparse matrix X and dictionary D are known, if d_k of the $k-th$ column of the dictionary D is modified, x_T^k is the $k-th$ line k of X, then the compensation term of formula (2) can be written as follows:

$$\left\|Y-DX\right\|_F^2 = \left\|Y-\sum_{j=1}^{K} d_j x_T^j\right\|_F^2 = \left\|\left(Y-\sum_{j\ne k}^{K} d_j x_T^j\right)-d_k x_T^k\right\|_F^2 = \left\|E_k - d_k x_T^k\right\|_F^2 \tag{3}$$

Define ψ recorded image block using atomic d_k Y samples, even when $x_T^k(i)$ is not 0 index value, then $\psi=\left\{i \mid 1\le i\le K, x_T^k(i)\ne 0\right\}$. On this basis, define the size of matrix $N\times\left|\psi\right|$ Ω_k, in $(\psi(i),i)$ value is 1, the other is 0. $x_R^k = x_T^k\Omega_k$, $E_k^R = E_k\Omega_k$ formula (3), and the transformation can be obtained:

$$\left\|E_k\Omega_k - d_k x_T^k\Omega_k\right\| = \left\|E_k^R - d_k x_R^k\right\| \tag{4}$$

Then amend the dictionary by the singular value decomposition of $E_k^R = U\Delta V^T$ on matrix E_k^R: using the first column of matrix U replaces the $k-th$ atom d_k of the dictionary, and using the first column of matrix V Multiplied by $\Delta(1,1)$ modifies x_R^k in formula (4), and then repeat the sparse representation and the modified process, until satisfied correction dictionary convergence conditions to obtain the ideal. The specific steps of the algorithm are as follows:

(1) Given a class of signal $Y=\left\{y_i\right\}_{i=1}^N$, standard dictionary $D^0 = R^{n\times K}$ as the initial dictionary, iteration $J=1$.

(2) Y is sparse representation by using dictionary D^0, which is to solve

$$\min_{x^i}\left\langle\left\|y_i - Dx_i\right\|_2^2\right\rangle, i=1,2,\cdots,N \qquad s.t. \qquad \left\|x_i\right\|_0 \le T_0$$

(3) Dictionary D^{J-1} is updated by atom, and the update step of atom d_k of column k is following:

1) Define step (2) by using k column atomic symbol set: $\omega_k=\left\{i \mid 1\le i\le N, x_T^k(i)\ne 0\right\}$

2) Calculate error matrix $E^k = Y - \sum_{j\ne k} d_j x_T^j$.

3) According to the elements of ω_k select the part of E^k as column E_R^k.

4) Singular value decomposition $E_k^R = U\Delta V^T$ for matrix E_k^R, use the first column of the matrix U to replace the k atom dictionary d_k, the first column using the matrix V and $\Delta(1,1)$ product as the coefficient of d_k.

(4) Return to step (2) repeat $J = J + 1$, until it is convergent.

Below is an optical image and SAR image obtained by K-SVD after training learned dictionary. Image block size is 8×8, the atomic number is 256.

(a) Optical image

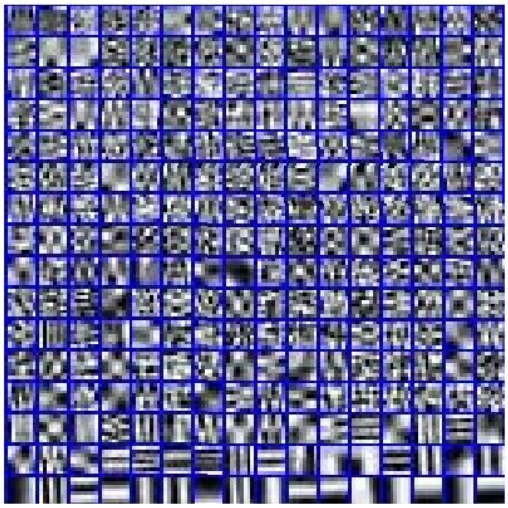

(b) Optical training dictionary

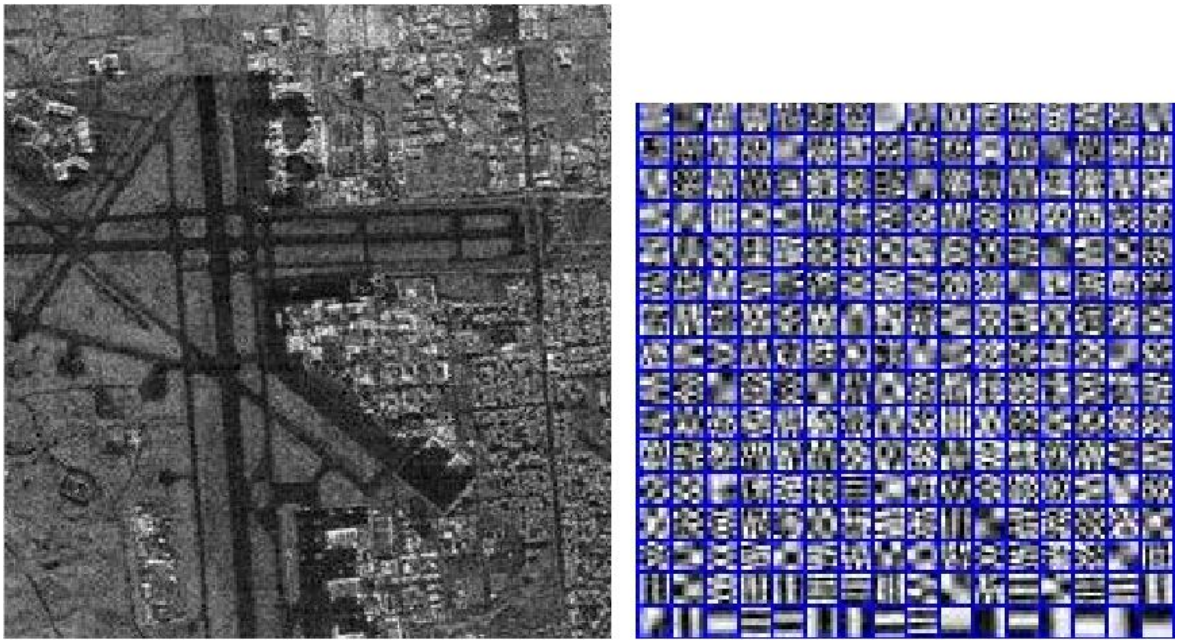

(c) SAR image (d) SAR training dictionary

Fig.2 K-SVD training dictionary

3.3 Orthogonal matching pursuit algorithm for sparse representation

Orthogonal matching pursuit algorithm (OMP) is used for sparse coding for image block, which the image block and the dictionary D are known, and calculate the process of image block of the sparse coefficient. It is a greedy pursuit algorithm, and the core idea is: first choose the nearest atom and image block from the dictionary, and calculate the residuals of the image blocks and the atom, and then select the approximate atom from the dictionary, and before the chosen atoms combined iterative approximation, iteration to residual less than a preset threshold. And orthogonal treatment of atoms in the iterative process is chosen to make the atoms not be reused.

In this process the image block fusion, sparse image block representation using OMP algorithm, the algorithm steps are as follows [23]:

Set the input image block for b, the dictionary for D , the sparse coefficient for X.

(1) Initialize the process, setting error ε, $X^0 = 0, r^0 = b, D_s^0 = \phi$;

(2) Select atom d_i from overcomplete dictionary which and is most close to signal b, namely d_i and b have the maximum inner product;

(3) The dictionary is updated $D_s^k = D_s^{k-1} \cup d_i$;

(4) Calculate the sparse coefficient X_s^k according to the atom library D_s^k;

(5) Calculate error $r^k = b - D_s^k X_s^k$;

(6) If $r^k \geq \varepsilon$, return step (2); Conversely, finish the cycle, and X_s^k is the sparse coefficient.

IV. FUSION ALGORITHM

4.1 Realization process of fusion algorithm

SAR images and optical images are fused based on the SVT fusion framework, and the low-frequency sub-band coefficients use the fusion method of the sparse representation to retain the good target information of SAR images, and the high-frequency sub-band coefficients are fused with the rules of the regional energy. The emphasis and difficulty of the algorithm is lied in the fusion of the low-frequency coefficients, and the paper does the are zero mean process to the image block to enhance the efficiency of sparse coding. The fusion process is shown in Fig.3, and the specific process is as follows[24]:

(1) The low-frequency images of SAR and optical images are divided into $n \times n$ image block by using sliding window , the step is $step \in [1, n]$, and then all the image blocks are changed into a column vector, and orderly image matrix $\{V_i^k\}_{i=1}^{[(M-n)/step+1][(N-n)/step+1]}$ $k \in \{1,2\}$, where V_i^1, V_i^2 denote the i SAR image and optical image columns, $[M, N]$ is the size of SAR images and optical images;

(2) V_i^k is done zero mean treatment, namely $V_i^k = V_i^k - mean\{V_i^k\}$. Then we use the OMP algorithm to do the sparse representation for vector V_i^k for each *i* position, so that we get the sparse coefficient $x_i^k, k \in \{1,2\}$;

(3) Fused coefficient x_i^k is gotten by the corresponding image block sparse coefficient x_i^f of SAR and optical images according to some fusion rules;

(4) All image blocks are done by step (2) and step (3) to obtain the fusion sparse coefficient matrix $\{x_i^f\}_{i=1}^{[(M-n)/step+1][(N-n)/step+1]}$, and then the fusion image is obtained via $V^F = D \times X^F + \overline{V^F}$ calculation, which D is gotten the dictionary $\overline{V^F} = (mean\{V_i^1\} + mean\{V_i^2\})/2$ by K-SVD training algorithm;

(5) The final low frequency fusion image can been gotten by the calculation of the location of various pixel mean on the basis of step (1).

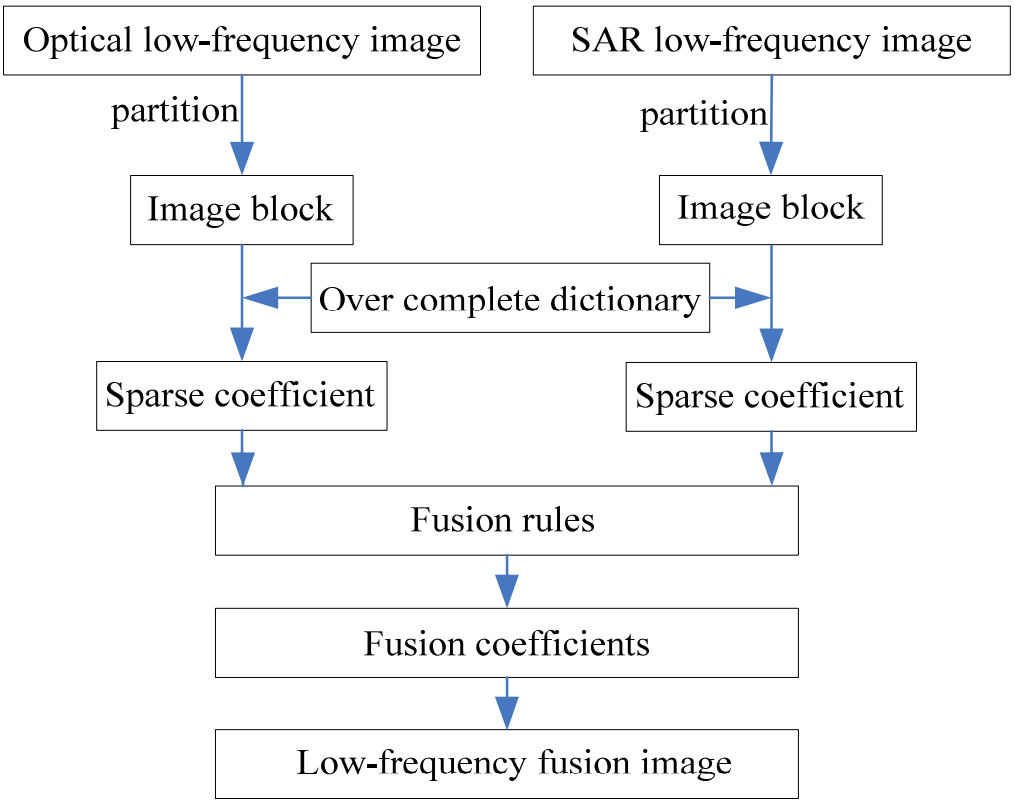

Fig.3 Flow chart of low-frequency image fusion

The selection of the fusion rule in step (3) is the most important part in the fusion method, which is a core factor in the final image fusion quality. Based on the sparse representation of the fusion algorithm proposed in the literature, using the l_1 norm sparse coefficient vector is adopted to obtain better fusion effect, which is the most commonly used sparse coefficients fusion rule. In this paper, by analyzing the characteristics of sparse coefficient, on the basis of reference [25], this paper proposes an adaptive weighted average and l_1 norm combining fusion rules.

4.2 Fusion rules

The coefficient vector is obtained by the image sparse decomposition, where l_1 norm reflects the image block activity, namely l_1 norm is more big, the more information is it [26]. If calculate the similarity S for fusion sparse coefficient vector l_1 norm , when the similarity of S is greater than the set threshold value T, it shows that the two fusion coefficient vector contains more information, using the weighted average of the information content of the two rules are effectively integrated. When the similarity of S is less than or equal to the threshold value T, it

shows that the coefficient vector contains the big difference in the information. In order to achieve a better fusion effect, it should use l_1 norm and rule fusion. Based on this, this paper presents a simple fusion rules combined with adaptive weighted average and l_1 norm. The specific calculation process is as follows:

(1) Assuming x_i^A and x_i^B are a sparse coefficient vector to fusion of SAR and optical frequency in the image, and it is calculated to get l_1 norm c_i^A and c_i^B by the following formula:

$$c_i^A = \left\| x_i^A \right\|_1 = \sum_{j=1}^{K} \left| x_{ij}^A \right| \tag{5}$$

$$c_i^B = \left\| x_i^B \right\|_1 = \sum_{j=1}^{K} \left| x_{ij}^B \right| \tag{6}$$

(2) Calculate similarity S_i of norm c_i^A and norm c_i^B of the fusing sparse coefficient vector l_1 by formula (5) and (6):

$$S_i = \frac{2 \cdot \sqrt{c_i^A c_i^B}}{c_i^A + c_i^B} \tag{7}$$

(3) Choose fusion rules according to the size of the similarity of S_i, and the fused coefficient vector is x_i^F:

When $S_i \geq T$:

$$x_i^F = \omega^A x_i^A + \omega^B x_i^B \tag{8}$$

Where ω^A and ω^B are respectively the corresponding weighted factor to be fusion coefficient vector, it can be calculated by the following formula:

$$\omega^A = c_i^A / \left(c_i^A + c_i^B \right) \tag{9}$$

$$\omega^B = 1 - \omega^A \tag{10}$$

When $S_i > T$:

$$x_i^F = \begin{cases} x_i^A & if \quad c_i^A \geq c_i^B \\ x_i^B & if \quad c_i^A < c_i^B \end{cases} \tag{11}$$

Where T is the threshold, and the experimental verification of $T \in [0.8,1]$ fusion effect is better, and this paper selects $T = 0.9$.

V. EXPERIMENTAL RESULTS AND ANALYSIS

In this paper, in order to verify the effectiveness of the algorithm, the traditional SVT based fusion method (SVT method) and the common fusion method based on sparse representation (SP method) are compared. In the algorithm of this paper, 10000 randomly selected image blocks as training samples are selected from 20 natural images, and obtain the overcomplete dictionary by using K-SVD algorithm. Image block size is 8×8, the dictionary size is 64×256, set the allowable error $\varepsilon = 0.01$ dictionary training $T = 10$, the sparsity of $T = 10$, step size $step = 4$. Operating environment for the experiments: computer CPU Pentium 4, 2.66GHz, 2GB memory, windows XP professional, a programming language for Matlab7.1. Here are two groups of SAR image and optical image for fusion effect verification, and the fusion results are shown in Fig.4 and Fig.5.

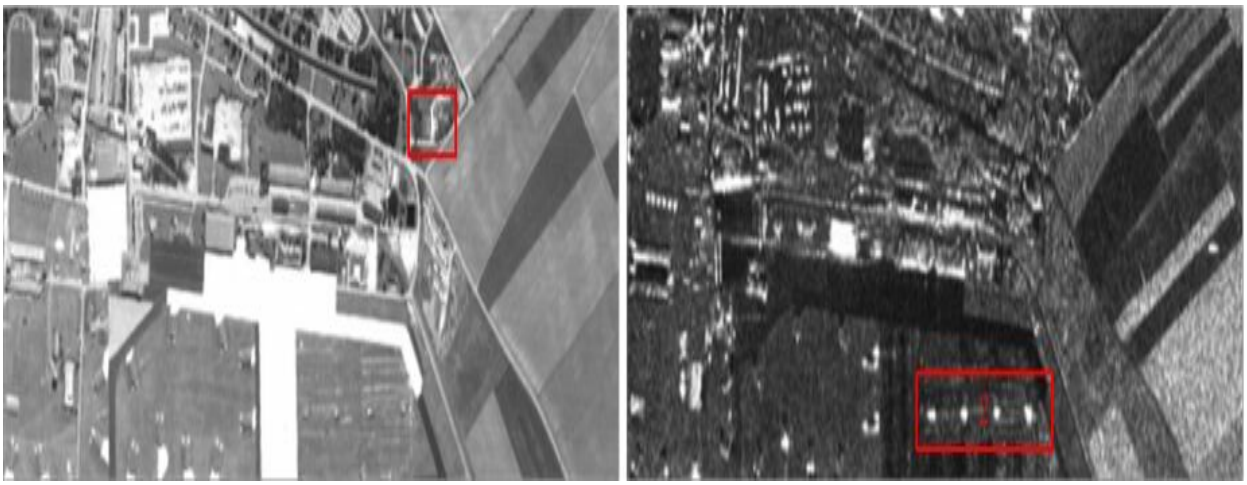

(a) Optical image (b) SAR

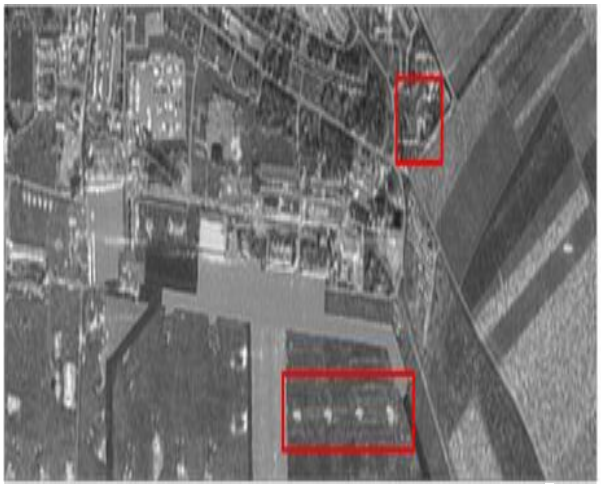

(c) Fusion results of SVT method

(d) Fusion results of SP method

(e) Fusion results of this method

Fig.4 Experimental results of the first set

(a) Optical image

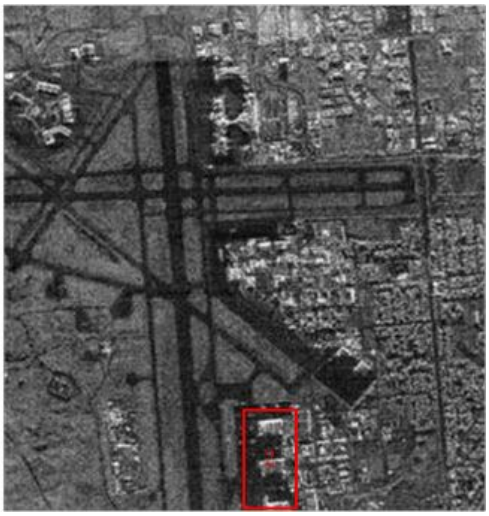

(b) SAR

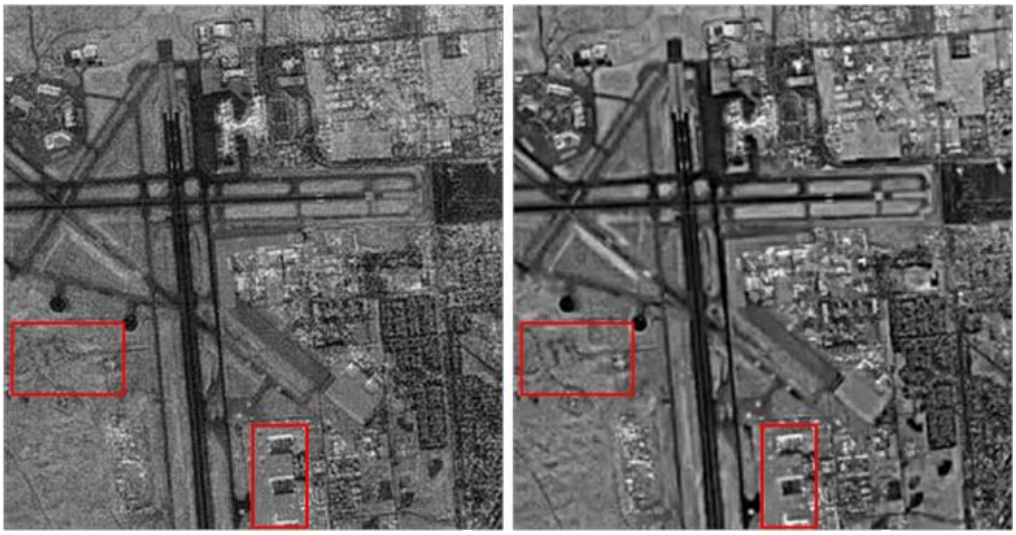

(c)Fusion results of SVT method (d) Fusion results of SP method

(e) Fusion results of this method

Fig.5 Experimental results of the second set

A. Subjective evaluation

(1) Compared with the source images

In fig.4 and fig.5, the fusion image and the source image are compared based on the two image information including the images of the house, the runway, grass etc..

(2) Comparison of three fusion images

From look on the whole, Fig.4 (c) has the minimum brightness, Fig.4 (e) has the highest brightness. It is seen from region 1, Fig.4 (d) has the worst ability maintaining the edge texture,

Fig.4 (e) has the most clear edge and texture. It is seen from the regional 2, Fig.4 (d) and Fig.3 (e) are well preserved in the SAR image information of the target. Therefore in the whole, Fig.4 (e) has the best visual effects. As you can see from Fig.5, Fig.5 (e) has the maximum brightness, clarity. In the target region 1, Fig.5 (e) has the most rich texture, and its clarity is the best. In the target region 2, Fig.5 (e) has the best target brightness, and it has the best target background contrast. Therefore, it has the best fusion method from the subjective evaluation.

B. Objective evaluation

For the quantitative evaluation of image fusion performance, here also to use standard deviation, entropy, average gradient and Piella index in Q_0, Q_E, Q_W and $Q^{AB/F}$ as a fusion quality evaluation index, using run time as the fusion efficiency evaluation index, the evaluation results in Figure .6 and Figure.7. In Figure .6 for the integration of objective evaluation index effect of the first group images, Figure .7 for the second groups of image fusion evaluation index.

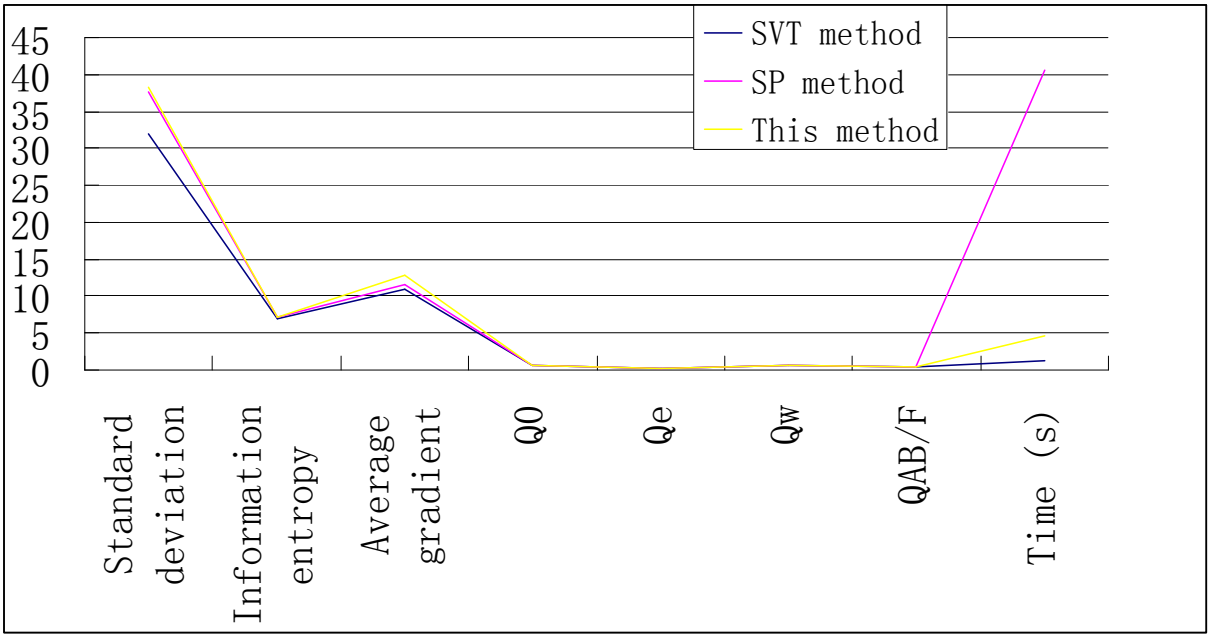

Figure 6.Objective evaluation indexes of the first set of image fusion

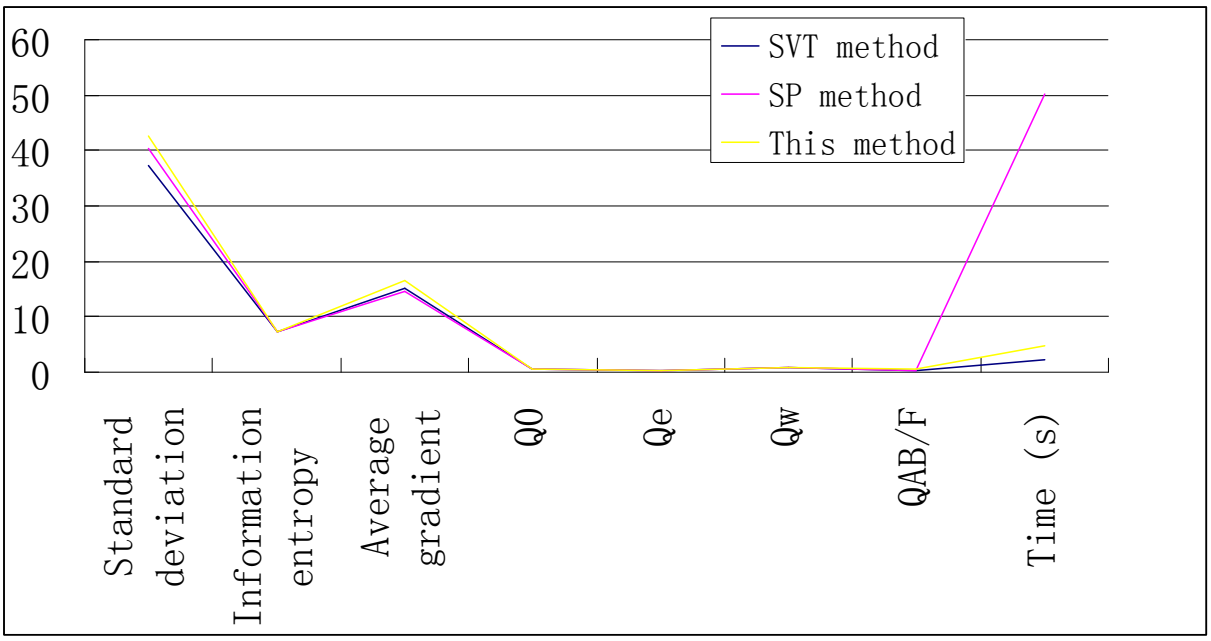

Figure .7 Objective evaluation indexes of the second set of image fusion

It can be seen from Figure .6 and Figure .7 , and the fusion indexes of SVT method and SP method have their pros and cons. While the algorithm in the paper is maximum in addition to running time, this is consistent with the subjective evaluation. Comparison of fusion and the method and the result of the SVT method, the standard deviations have increased by 20.72% and 14.43% in Table.1 and Table.2, and the information entropy is increased by 3.31% and 2.35%, and average gradient is increased by 16.60% and 9.71%, and the average Piella index is increased by 11.56% and 7.97%. Overall, the quality of both average indexes is increased, and it fully is proved the superiority of the algorithm in this paper. From operating efficiency, the running time of this algorithm is lower than the conventional SP algorithm, which shows the effectiveness of the improved algorithm in this paper.

VI. CONCLUSION

Obtain the following conclusion through the experiment: (1) The multi-scale decomposition and sparse representation by using the combination of SAR image and Optical image fusion, the decomposition algorithm is better effect than conventional multi-scale fusion. (2) It enhances the efficiency of sparse decomposition by the treatment of zero mean image block. (3) The paper proposes a sparse coefficient fusion rule based on the adaptive weighted average and l_1 norm,

and it is fit for the image fusion of SVT slow-frequency decomposition of the optical image and SAR image, and the experimental results demonstrate the effectiveness of the fusion rule.

VII. REFERENCES

[1] Wang Wen-cheng, Chang Fa-liang. A Multi-focus Image Fusion Method Based on Laplacian Pyramid, Journal of Computers, 2011, 6 (11): 2559-2566.

[2] A. Baradarani, Jonathan Q M, M. Ahmadi, et al. Tunable half band-pair wavelet filter banks and application to multi-focus image fusion, Pattern Recognition, 2012, 45 (2): 657-671.

[3] Sale, D.; Patil, V. ; Joshi, M.A, Effective image enhancement using hybrid multi resolution image fusion, 2014 IEEE Global Conference on Wireless Computing and Networking (GCWCN), pp.116 - 120, 2014.

[4] Wei Huan-ga, Jing Zhong-liang, Evaluation of focus measures in multi-focus image fusion, Pattern Recognition Letters, 2007, 28 (4): 493-500.

[5] Iuliia Shatokhina, Andreas Obereder, Matthias Rosensteiner, et al, Preprocessed cumulative reconstructor with domain decomposition: a fast wave-front reconstruction method for pyramid wave-front sensor [J]. Applied Optics, 2013, 52 (12): 2640-2652.

[6] Aritra Sengupta, Noel Cressie, Hierarchical statistical modeling of big spatial datasets using the exponential family of distributions [J]. Spatial Statistics, 2013, 4 (1): 14-44.

[7] Harikumar, V. et al., Multi-resolution Image Fusion: Use of Compressive Sensing and Graph Cuts, IEEE Journal of Selected Topics in Applied Earth Observations and Remote Sensing, vol.7, no.5, pp.1771 - 1780, 2014.

[8] Upla, K.P. ; Joshi, M.V. ; Gajjar, P.P., An Edge Preserving Multiresolution Fusion: Use of Contourlet Transform and MRF Prior, IEEE Transactions on Geoscience and Remote Sensing, vol.53, no.6, pp.3210 - 3220, 2015.

[9] Min Li, Gang Li, Wei Cai, Xiao-yan Li. A Novel Pixel-Level and Feature-Level Combined Multisensor Image Fusion Scheme, Lect. Notes in Computer Science, 2008, 52 (1): 658-665.

[10] Benjamin W. Martin, Ranga R. Vatsavai. Evaluating fusion techniques for multi-sensor satellite image data, Proc. of SPIE Vol, 2013 (8747), 87470J.

[11] Xing Su-xia, Lian Xiao-feng,Chen Tian-hua, et al, Image Fusion Method Based on NSCT and Robustness Analysis, 2011 International Conference on Computer Distributed Control and Intelligent Environmental Monitoring, 2011: 346-349.

[12] Bin Yang, Shutao Li, Pixel-level image fusion with simultaneous orthogonal matching pursuit, Information Fusion,2012,13(1):10-19.

[13] Zhou Wang, Bovik AC, A Universal Image Quality Index, IEEE Signal Processing Letters, 2002, 9 (3): 81-84.

[14] Piella G, Heijmans H. Anew quality metric for image fusion[C]. The International Conference on Image Processing, 2003, 3: 173-176.

[15] Shuang Li, Zhilin Li, Jianya Gong, Multivariate statistical analysis of measures for assessing the quality of image fusion[J]. International Journal of Image and Data Fusion, 2010, 1 (1): 47-66.

[16] Susanta Mukhopadhyay, Bhabatosh Chanda, Fusion of 2D gray-scale images using multi-scale Morphology[J]. Pattern Recognition, 2001, 34 (10): 1939-1949.

[17] Xiangzhi Bai. Image fusion through feature extraction by using sequentially combined toggle and Top-Hat based contrast operator [J]. Applied Optics, 2012, 51 (31): 7566-7575.

[18] Yang B. and Li S. T. Pixel-level image fusion with simultaneous orthogonal matching pursuit, Inf. Fusion. 2012, 13 (1): 10-19.

[19] Jun Wang, Jinye Peng, Xiaoyi Feng, et al. Image fusion with non-subsampled contourlet transform and sparse representation, Journal of Electronic Imaging, 2013, 22 (4): 1-15.

[20] Aharon M, Elad M, Bruckstein AM, The K-SVD: An algorithm for designing of over-complete dictionaries for sparse representations, IEEE Tran. Image Process, 2006, 54 (11): 4311-4322.

[21] Yang J Y, Peng Y G, Xu W L, et al. Ways to sparse representation: an overview, Science in China Series F: Information Sciences, 2009, 52 (4): 695-703.

[22] Yang B, Li S T. Multi-focus Image Fusion and Restoration with Sparse Representation, IEEE Transactions on Instrumentation and Measurement, 2010, 59 (4): 884-892.

[23] Liqiang Guo, Ming Dai, Ming Zhu, Multi-focus color image fusion based on quaternion curvelet transform, 2012, 20 (17): 18846-18860.

[24] Erik Reinhard , Michael Ashikhmin, Bruce Gooch , Peter Shirley. Color Transfer between images, IEEE Computer Graphics and Applications, 2001, 21 (5): 34-41.

[25] Takashi Kondo, Xiaohua Zhang, Coloring of Gray Scale Image Using Image Color Transfer, The Journal of The Institute of Image Information and Television Engineers, 2007, 61 (6): 838-841.

[26] Toet A, Franken E M. Perceptual evaluation of different image fusion schemes [J]. Displays, 2003, 24 (1): 25-37.

[27] David Blacknell ; Nicholas S. Arini ; Ian McConnell, SAR image understanding using contextual information, Proc. SPIE 4543, SAR Image Analysis, Modeling, and Techniques IV, vol. 4543, pp. 73-84,2002.

[28] Xixi Huang, Xiaofeng Wang, The Classification of Synthetic Aperture Radar Oil Spill Images Based on the Texture Features and Deep Belief Network, Lecture Notes in Electrical Engineering, vol.277, pp 661-669, 2014.

[29] N. K. Suryadevara, S. C. Mukhopadhyay. R.K. Rayudu and Y. M. Huang, Sensor Data Fusion to determine Wellness of an Elderly in Intelligent Home Monitoring Environment, Proceedings of IEEE I2MTC 2012 conference, IEEE Catalog number CFP12MT-CDR, ISBN 978-1-4577-1771-0, May 13-16, 2012, Graz, Austria, pp. 947-952.

[30] Yueting Zhang, Chibiao Ding, Hongzhen Chen, Hongqi Wang, Special Phenomena of the Shadow Region in the High Resolution Synthetic Aperture Radar Image due to Synthetic Aperture, Journal of Infrared, Millimeter, and Terahertz Waves, Volume 33, Issue 10, pp 1052-1070, 2012.

[31] Wei Liang, S.C. Mukhopadhyay, Rajali Jidin and Chia-Pang Chen, Multi-Source Information Fusion for Drowsy Driving Detection Based on Wireless Sensor Networks, Proceedings of the 2013 7th International Conference on Sensing Technology, ICST 2013, December 3-5, 2013, Wellington, New Zealand, pp. 861-868, ISBN 978-1-4673-5221-5.

[32] Wisnu Jatmiko, Ikhsanul Habibie, et al., Automated telehealth system for fetal growth detection and approximation of ultrasound images, International Journal on Smart Sensing and Intelligent Systems, 8(1), pp.697 − 719, 2015.

[33] S. Bhardwaj, D. S. Lee, S.C. Mukhopadhyay, and W. Y. Chung, A Fusion Data Monitoring of Multiple Wireless Sensors for Ubiquitous Healthcare System, Proceedings of the 2nd International Conference on Sensing Technology Nov. 26-28, 2007 Palmerston North, New Zealand, pp. 217-222.

[34] Chastine Fatichah, Diana Purwitasari, et al., Overlapping white blood cell segmentation and counting on microscopic blood cell images, International Journal on Smart Sensing and Intelligent Systems, 7(4), pp. 1271 − 1286, 2014.